NANO LETTERS

Letter

pubs.acs.org/NanoLett

Vibrational Spectroscopic Observation of Atomic-Scale Local Surface Sites Using Site-Selective Signal Enhancement

Jian Hu,[†,‡] Nagahiro Hoshi,[§] Kohei Uosaki,[‡,∥] and Katsuyoshi Ikeda*[,†,‡,⊥]

[†]Division of Chemistry, Graduate School of Science, Hokkaido University, Sapporo 060-0810, Japan

[‡]Global Research Center for Environment and Energy Based on Nanomaterials Science (GREEN), National Institute for Materials Science (NIMS), Tsukuba 305-0044, Japan

[§]Department of Applied Chemistry and Biotechnology, Graduate School of Engineering, Chiba University, Yayoi-cho 1-33, Inage-ku, Chiba 263-8522, Japan

[∥]International Center for Materials Nanoarchitectonics (WPI-MANA), National Institute for Materials Science (NIMS), Tsukuba 305-0044, Japan

[⊥]Japan Science and Technology Agency, PRESTO, 4-1-8 Honcho, Kawaguchi, Saitama 332-0012, Japan

Supporting Information

ABSTRACT: Molecule−substrate interactions are sensitively affected by atomic-scale surface structures. Unique activity in heterogeneous catalysts or electrocatalysts is often related with local surface sites with specific structures. We demonstrate that adsorption geometry of a model molecule with an isocyanide anchor is drastically varied among one-fold atop, two-fold bridge, and three-fold hollow configurations with increasing the size of atomic-scale local surface sites of Pd islands on an Au(111) model surface. The vibrational spectroscopic observation of such local information is realized by site-selective and self-assembled formation of hotspots, where Raman scattering intensity is significantly enhanced via excitation of localized surface plasmons.

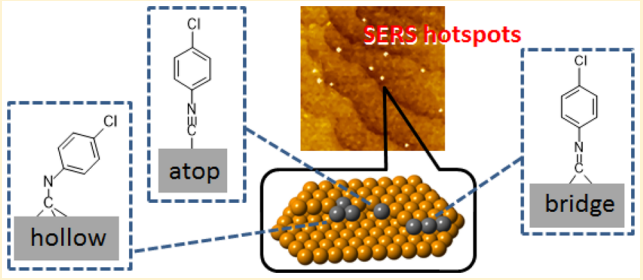

KEYWORDS: *Atomic-scale surface defects, surface enhanced Raman scattering, localized surface plasmon resonance, metal−molecule interactions*

In heterogeneous catalysts and electrocatalysts, interactions between reactant molecules and a catalytic substrate are sensitively affected by its geometric and electronic surface properties.[1] To understand such interactions, atomically defined single crystalline model surfaces of various orientations have been employed in both spectroscopic and electrochemical investigations.[2,3] The formation of foreign metal overlayers on a metal surface has also been extensively studied as a key technique to tune catalytic activity.[4−7] The use of such well-defined and uniform model surfaces can provide valuable insights on the relation between the surface structure and activity. However, very limited information is currently available regarding local surface sites such as surface defects or surface impurities, which may exhibit unique catalytic properties.[8] Here we demonstrate that local information on molecular geometries adsorbed on atomic model surface sites can be observed using site-selective and self-assembled formation of hotspots, where Raman scattering intensity is significantly enhanced via excitation of localized surface plasmons. It is presented that molecule−substrate interactions are critically sensitive to the atomic-scale surface structures.

Vibrational spectroscopies do not routinely provide surface-specific information on catalytic substrates. Improved techniques such as surface enhanced vibrational spectroscopy[9−11] or second order nonlinear optical spectroscopy[12] can realize surface-selective observations. However, these methods typically deliver only averaged information on molecular adsorbates at various surface sites exposed, due to the diffraction-limited spatial resolution of submicrometer order. Among the surface sensitive spectroscopies, surface enhanced Raman spectroscopy, SERS, has the potential to break the diffraction limit because the signal enhancement occurs only in the vicinity of metal nanostructures. Nanomapping of dye molecules or carbon nanotubes has already been demonstrated using the advanced SERS technique with a metallized scanning probe, which is known as tip enhanced Raman scattering (TERS).[13,14] Unfortunately, such molecularly resolved vibrational imaging is technically difficult, especially when target molecules are electronically off-resonant with the excitation light.[15,16] The use of a single hotspot at the tip end limits the gain of the overall signal intensity, which results in poor signal-to-noise ratio in the spectra. In addition, the excess excitation intensity may cause

Received: August 5, 2015
Revised: October 21, 2015
Published: November 9, 2015

DOI: 10.1021/acs.nanolett.5b03093
Nano Lett. 2015, 15, 7982−7986

damage to the sample. If a number of hotspots are created only on specific local surface sites, spectroscopic information on local sites can be obtained selectively.

In the field of surface electrochemistry, the high-index stepped surfaces of single crystalline metals are frequently utilized as a model electrocatalyst surface with monatomic steps, which can be considered as regulated local surface sites.[17,18] However, the electrochemical response of such surfaces involves responses of the terraces as well as those of the steps. For the conventional SERS spectroscopy, moreover, such an atomically smooth model surface is out of consideration because nanostructured or roughened metal surfaces are utilized as a SERS-active substrate. Recently, sphere-plane type plasmonic nanostructures have drawn much attention in the SERS community because they enable observation of SERS-inactive planar metal surfaces, including the catalytic Pt group metals.[19−24] In this technique, a number of SERS hotspots are created on a metal substrate by assistance of Au nanoparticles (AuNPs); when an AuNP is nearly in touch with a metal substrate, significant enhancement of Raman scattering intensity occurs only in the NP−substrate gap through excitation of the so-called gap-mode plasmons.[25,26] That is, each AuNP can function as a SERS hotspot on the metal surface. Hereinafter, this SERS system is referred to as NP-assisted gap-mode SERS. This technique is particularly useful for observing organic monolayers adsorbed on a metal surface because the well-defined nanogaps can be easily formed by direct attachment of AuNPs on top of the monolayer-covered metal surface.[19,20] Here, the adsorption of AuNPs on the organic layer is mainly caused by van der Waals interactions between AuNPs and molecular adsorbates. We have already performed NP-assisted gap-mode SERS observation of various low- and high-index faces of single crystalline metals to study metal−molecule interactions,[27−29] although the information from both terraces and steps was involved in the spectra, as expected. The remaining issue to realize site-selective SERS observation is how AuNPs can be selectively adsorbed on specific local sites. In this work, atomic Pd islands on Au(111) face were utilized as a model of local surface sites, and SERS hotspots were created only on Pd islands using preferential adsorption of AuNPs.

First, a conventional (111)-cut Au surface was utilized to demonstrate site-selective SERS observation. Experimental details are described in Supporting Information. The polished and annealed surface has many mechanical scratches, which may act as uncontrolled defects (see Figure S1). Pd was partially electrodeposited on the surface to form local model surface sites. Figure 1a shows a negative-going linear potential sweep voltammogram for underpotential deposition of Pd on the (111)-cut Au surface (Pd-UPD). Nucleation of such Pd monolayers preferentially occurs at energetically favored sites, so that the first reduction peak at around 0.6 V vs Ag/AgCl is assigned to UPD at defect sites, whereas the second peak at 0.57 V is assigned to UPD at terraces.[30] Two types of Pd (sub)monolayers with different coverages of 0.8 ML ($Pd_{0.8\ ML}$) and 0.03 ML ($Pd_{0.03\ ML}$) were prepared on the Au(111) surfaces by potential application of 0.57 and 0.65 V vs Ag/AgCl, respectively. The $Pd_{0.03\ ML}$ islands are expected to be formed only at the defect sites, while the $Pd_{0.8\ ML}$ overlayer covers both defects and terraces. Self-assembled molecular monolayers of a model adsorbate, 4-chlorophenyl isocyanide (CPI), were then formed on these surfaces. Vibrational spectra of the adsorbed molecules before and after deposition of

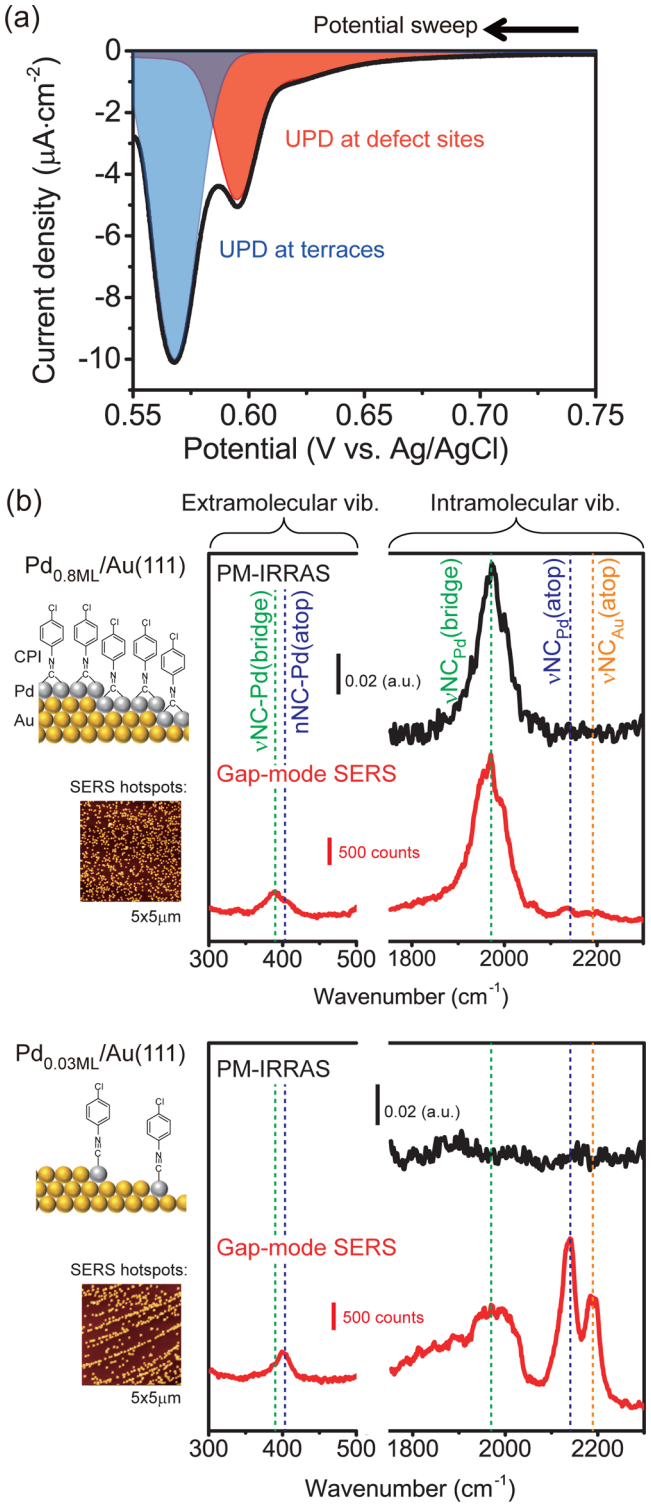

Figure 1. Electrochemical surface modification of a (111)-cut Au surface with Pd atoms and vibrational spectroscopic observations of the modified surfaces. (a) Negative-direction linear potential sweep voltammogram for Pd-UPD on a (111)-cut Au surface. (b) PM-IRRAS and NP-assisted gap-mode SERS spectra for CPI on $Pd_{0.8\ ML}$/Au(111) and $Pd_{0.03\ ML}$/Au(111). The vertical axes for PM-IRRAS and SERS are expressed as PM-IRRAS signal intensity (a.u.) and Raman scattering intensity (counts), respectively. Schematic illustrations of these surfaces and typical AFM images are also presented on the left-hand side of the figure.

DOI: 10.1021/acs.nanolett.5b03093
Nano Lett. 2015, 15, 7982−7986

AuNPs were measured using polarization modulation infrared reflection absorption spectroscopy (PM-IRRAS) and NP-assisted gap-mode SERS, respectively. For the SERS measurements, citrate-capped AuNPs with diameter of ca. 50 nm were physisorbed by immersion of the samples into colloidal solution of AuNPs.

For $Pd_{0.8\ ML}$ (Figure 1b, top panel), the atomic force microscopy (AFM) image shows that the adsorbed AuNPs, i.e., the SERS hotspots, are homogeneously distributed over the entire surface. Both PM-IRRAS and SERS spectra showed a distinct peak at 1971 cm^{-1} in the intramolecular vibrational region, which corresponds to the stretching mode of the NC anchor group bound to Pd with a bridge configuration (νNC_{Pd}(bridge)).[30] The absence of the vibration mode for NC bound to Au (νNC_{Au}) indicates that the CPI monolayers remain intact, even after the deposition of AuNPs. However, the AFM image for $Pd_{0.03\ ML}$ (Figure 1b, bottom panel) indicates that the SERS hotspots are created only around the surface scratches, which were covered with Pd islands. The AuNPs can be adsorbed onto CPI monolayers through van der Waals interactions; therefore, the inhomogeneous distribution of adsorbed AuNPs implies that the surface density of CPIs is also inhomogeneous. In other words, the surface distribution of CPI was successfully transferred to that of AuNPs. PM-IRRAS could not detect any vibrational peak, which suggests that the total amount of CPI on the $Pd_{0.03\ ML}$ islands was under the detection limit. Nevertheless, the gap-mode SERS spectrum clearly showed three vibrational peaks of CPI in the intramolecular vibrational region; the broad peak at around 1980 cm^{-1} is ascribed to νNC_{Pd}(bridge), and the other peaks at 2140 and 2190 cm^{-1} can be assigned to the stretching modes of NC groups with atop configurations bound to Pd (νNC_{Pd}(atop)) and Au (νNC_{Au}(atop)) sites, respectively.[31] The appearance of νNC_{Au}(atop) on $Pd_{0.03\ ML}$ is presumably due to the adsorption of CPI on Pd-uncoated defect sites of the Au(111) substrate. However, the presence of νNC_{Pd}(bridge) and νNC_{Pd}(atop) indicates that CPI is preferentially adsorbed on Pd atoms than on Au atoms on the Pd/Au mixed surface. The dominant molecular geometry is dependent on the Pd-coverage: atop on $Pd_{0.03\ ML}$ and bridge on $Pd_{0.8\ ML}$. This difference is also observed in the extramolecular vibrational region, where the stretching mode of the NC-Pd bond was around 400 cm^{-1} on $Pd_{0.03\ ML}$ and around 380 cm^{-1} on $Pd_{0.8\ ML}$. The former can be assigned to νNC-Pd(atop) and the latter to νNC-Pd(bridge). Therefore, it is clear that the local molecular information on Pd islands can be obtained using NP-assisted gap-mode SERS technique.

To investigate the details of molecule−metal interactions at specific surface sites, conventional (111)-cut surfaces are not of sufficient quality, even though such surfaces are commonly accepted as "well-defined" surfaces for electrochemical experiments (see details in Supporting Information). Instead, we have employed a carefully annealed (111) facet of single crystalline Au microbeads. Figure 2a (left panel) shows a typical AFM image of such an Au(111) facet with monatomic steps and micrometric terraces. After deposition of the AuNPs on this Au(111) surface with partial coating of Pd and CPI, the AFM image shows that the deposited AuNPs are located near the step lines, where the surface density of atomic defects are relatively high (Figure 2a, right panel). It should be noted again that the initial nucleation in Pd-UPD is expected to occur only at defect sites. The size of Pd islands can be varied by tuning of the UPD potential within the range of the first deposition peak

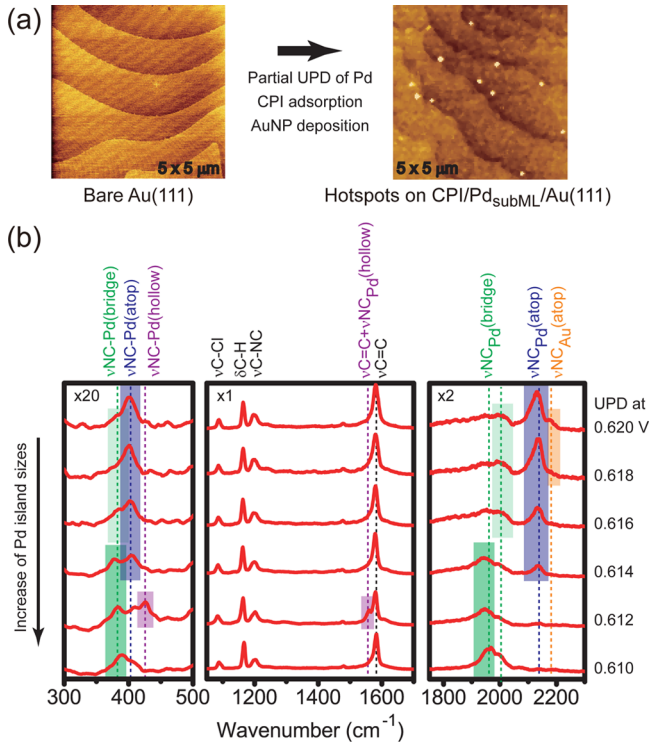

Figure 2. (a) (left) AFM image of an Au(111) facet with micrometric width terraces, and (right) AFM image of AuNPs deposited on the facet partially covered with Pd and CPI. (b) NP-assisted gap-mode SERS spectra for CPI on Au(111) facets with various Pd coverage. It is expected that Pd islands were formed only at the edge of monatomic step lines. All spectra were normalized according to the δC−H peak intensity.

in Figure 1a; due to the evolution of the islands, the sizes are expected to be larger with a negative shift of the potential. Such nucleation and evolution of Pd islands has been observed using *in situ* scanning tunneling microscopy (STM).[30]

Figure 2b shows NP-assisted gap-mode SERS spectra of CPI molecules measured on a series of Pd-UPD/Au(111) facets formed by application of various electrochemical potentials. For a UPD potential of 0.62 V, the spectral appearance was very close to that for the $Pd_{0.03\ ML}$ islands on the (111)-cut Au surface in Figure 2b. However, for the more negative potential at 0.61 V, the spectral feature was rather similar to that for $Pd_{0.8\ ML}$. The potential of 0.61 V was not sufficient to initiate UPD at the terraces; therefore, the observed spectral change indicates that the molecular adsorption geometry is quite sensitive to the size of the Pd islands. (Although Au surfaces may be restructured on the atomic scale by adsorption of isocyanide molecules,[32] one can exclude a possibility that the observed spectral change was induced by the interactions between Au and CPI because Pd-covered surface sites were formed before the adsorption of CPI and then site-selective observation was conducted on the Pd sites.) The preferential adsorption geometry evolves from the atop to bridge configurations in the potential region between 0.62 and 0.61 V, as shown by both the νNC_{Pd} and νNC-Pd vibration modes. In addition to this significant spectral variation, two additional potential dependences are noted. One is the frequency shift of νNC_{Pd}(bridge) from ca. 2000 to 1950 cm^{-1}, which is correlated with the decrease in νNC_{Pd}(atop). The other is that the hollow adsorption of CPI is observed only for a specific condition of

DOI: 10.1021/acs.nanolett.5b03093
Nano Lett. 2015, 15, 7982−7986

the Pd islands, which can be confirmed by the appearance of νNC_{Pd}(hollow) at 1560 cm^{-1} and νNC-Pd(hollow) at 425 cm^{-1}. It should be noted that this behavior of the hollow configuration was reproducible for several experiments, although the exact coverage of Pd on the Au(111) facet was not obtained; the hanging-meniscus electrochemical configuration was not maintained for the facet formed on a spherical monocrystalline bead.

The initial stage of Pd-UPD on Au(111) may be illustrated as shown in Figure 3. The nucleation of Pd-UPD preferentially

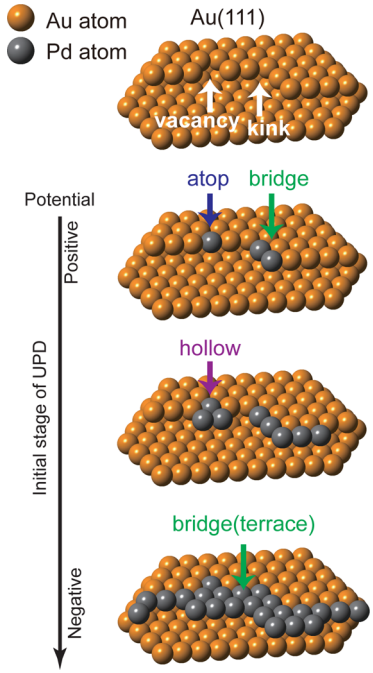

Figure 3. Schematic illustration of Pd nucleation at the initial stage of UPD. Isolated Pd atomic monomers, dimers, and trimers at defect sites of Au(111) can be adsorption sites with atop, bridge, and hollow configurations, respectively. The atop adsorption is dominant at the beginning of Pd-UPD. When Pd coating at step lines is completed, bridge adsorption becomes dominant. However, at a certain coverage of Pd, the hollow configuration becomes preferential, which suggests that a unique local surface feature appears with a specific size of Pd islands.

occurs at defects such as step vacancies or kink sites, which results in the formation of isolated Pd atomic monomers or dimers.[30] It is naturally expected that CPI is adsorbed with the atop configuration on Pd monomer sites due to the geometric limitation. However, for Pd dimer sites, the bridge configuration also becomes possible. Similar adsorption behavior has also been reported for carbon monoxide adsorbed on Pd atomic monomers on a Pd/Au alloy surface using IRRAS observations.[33] In the present case, the bridge configuration is energetically more favorable on a continuous Pd film than the atop configuration. Hence, the increase of the Pd island sizes, i.e., the decrease in the surface density of Pd monomers, can result in evolution from νNC_{Pd}(atop) to νNC_{Pd}(bridge), as shown in Figure 2b. For νNC_{Pd}(bridge), the peak shift from 2000 to 1950 cm^{-1} was also observed in correlation with the decrease in the νNC_{Pd}(atop) intensity. The frequency change in the NC bridge configuration is generally related to the change in the degree of π-back-donation between the d-orbital of Pd and the π^*-orbital of NC.[28] Therefore, the observed peak shift is expected to reflect the difference in the environmental conditions around Pd dimers; the νNC_{Pd}(bridge) at around 2000 cm^{-1} is presumably originated from CPI molecules adsorbed on Pd atoms interacting with Au step edges, while the νNC_{Pd}(bridge) at around 1950 cm^{-1} is attributed to those on Pd atoms apart from Au steps.

During the growth of Pd islands, there is a possibility for Pd atomic trimers to appear in an isolated manner, as illustrated in Figure 3. The observed νNC_{Pd}(hollow) may be due to adsorption on such isolated local sites. However, this type of local site would easily disappear during further deposition of Pd. Eventually, the hollow configuration can appear only at a specific UPD condition, and the bridge configuration is finally dominant on a continuous Pd monatomic film. This assumption is supported by an additional experiment using a high-index Au(311) surface (see Supporting Information). Accordingly, it is strongly suggested that the interaction of Pd local sites with molecules are significantly varied with an increase of the size of the islands at the atomic scale, although the interpretation of the spectra must be further examined using other theoretical and experimental methods.

Surface modification of a metal surface using foreign metals is a promising strategy to improve catalytic performance. However, the spectroscopic investigations of small amounts of local surface sites are still limited by the lack of experimental techniques. When the size of the islands is down to the atomic scale, their properties become rather complicated and more sensitive to the local environment of the substrate. As such, pronounced catalytic activity for the hydrogen evolution reaction has been reported when Au(111) steps are partially coated with Pd atoms.[8] Such modification is very difficult to control on a conventional substrate; therefore, the relation between the activity and the local surface features remains under discussion.[34] Although the Pd/Au alloy surface may be considered as a model of local surface sites,[33] the surface electronic nature should be different from that of Pd islands on the bulk Au substrate. The present experiment provides more straightforward vibrational information on local surface sites. The key issue in this technique is that site-selective signal enhancement is realized by site-selective and self-assembled formation of SERS hotspots through van der Waals interactions between AuNPs and the molecular adsorbates. Thus, the spatial differences in substrate−molecule interactions were amplified in the SERS spectra through local signal enhancement. The present method will be particularly useful for investigations of well-defined local surface sites on atomically controlled model surfaces, which is expected to lead to the design of superior catalysts with the desired surface structures.

■ ASSOCIATED CONTENT

Supporting Information

The Supporting Information is available free of charge on the ACS Publications website at DOI: 10.1021/acs.nanolett.5b03093.

Further details about experimental methods, (111)-cut surface vs (111) facet of Au single crystals, and NP-assisted gap-mode SERS spectrum of CPI on Pd full-covered (311)-cut Au surface (PDF)

■ AUTHOR INFORMATION

Corresponding Author

*E-mail: kikeda@nitech.ac.jp.

DOI: 10.1021/acs.nanolett.5b03093
Nano Lett. 2015, 15, 7982−7986

Present Address
(K.I.) Frontier Research Institutes for Materials Science (FRIMS), Nagoya Institute of Technology, Gokiso, Showa, Nagoya 466-8555, Japan.

Notes
The authors declare no competing financial interest.

■ ACKNOWLEDGMENTS

This research was supported in part by a Grant-in-Aid for Young Scientists (A) (No. 24681018) from the Japan Society for the Promotion of Science (JSPS), World Premier International Research Center (WPI) Initiative on Materials Nanoarchitectonics, and the Program for Development of Environmental Technology using Nanotechnology of the Ministry of Education, Culture, Sports, Science and Technology (MEXT), Japan.

■ REFERENCES

(1) Wieckowski, A., Ed. *Interfacial Electrochemistry: Theory, Experiment, and Applications*; Marcel Dekker: New York, 1999.
(2) Markovic, N. M.; Ross, P. N. *Surf. Sci. Rep.* **2002**, *45*, 117−229.
(3) Alkire, R. C.; Kolb, D. M.; Lipkowski, J.; Ross. P. M., Eds. *Diffraction and Spectroscopic Methods in Electrochemistry*; Wiley-VCH: Weinheim, Germany, 2006.
(4) Hammer, B.; Nørskov, J. K. *Adv. Catal.* **2000**, *45*, 71−129.
(5) Kibler, L. A.; El-Aziz, A. M.; Hoyer, R.; Kolb, D. M. *Angew. Chem., Int. Ed.* **2005**, *44*, 2080−2084.
(6) Naohara, H.; Ye, S.; Uosaki, K. *Electrochim. Acta* **2000**, *45*, 3305−3309.
(7) Stamenkovic, V. R.; Mun, B. S.; Arenz, M.; Mayrhofer, K. J. J.; Lucas, C. A.; Wang, G.; Ross, P. N.; Markovic, N. M. *Nat. Mater.* **2007**, *6*, 241−247.
(8) Kibler, L. A. *ChemPhysChem* **2006**, *7*, 985−991.
(9) Fleischmann, M.; Hendra, P. J.; McQuillan, A. J. *Chem. Phys. Lett.* **1974**, *26*, 163−166.
(10) Hartstein, A.; Kirtley, J. R.; Tsang, J. C. *Phys. Rev. Lett.* **1980**, *45*, 201−204.
(11) Osawa, M.; Ikeda, M. *J. Phys. Chem.* **1991**, *95*, 9914−9919.
(12) Zhu, X. D.; Suhr, H.; Shen, Y. R. *Phys. Rev. B: Condens. Matter Mater. Phys.* **1987**, *35*, 3047−3050.
(13) Hartschuh, A.; Sánchez, E. J.; Xie, X. S.; Novotny, L. *Phys. Rev. Lett.* **2003**, *90*, 095503.
(14) Steidtner, J.; Pettinger, B. *Phys. Rev. Lett.* **2008**, *100*, 236101.
(15) Liu, Z.; Ding, S.-Y.; Chen, Z.-B.; Wang, X.; Tian, J.-H.; Anema, J. R.; Zhou, X.-S.; Wu, D.-Y.; Mao, B.-W.; Xu, X.; Ren, B.; Tian, Z.-Q. *Nat. Commun.* **2011**, *2*, 305.
(16) Zhang, R.; Zhang, Y.; Dong, Z. C.; Jiang, S.; Zhang, C.; Chen, L. G.; Zhang, L.; Liao, Y.; Aizpurua, J.; Luo, Y.; Yang, J. L.; Hou, J. G. *Nature* **2013**, *498*, 82−86.
(17) Lecoeur, J.; Andro, J.; Parsons, R. *Surf. Sci.* **1982**, *114*, 320−330.
(18) Hoshi, N.; Kuroda, M.; Koga, O.; Hori, Y. *J. Phys. Chem. B* **2002**, *106*, 9107−9113.
(19) Ikeda, K.; Fujimoto, N.; Uehara, H.; Uosaki, K. *Chem. Phys. Lett.* **2008**, *460*, 205−208.
(20) Ikeda, K.; Sato, J.; Fujimoto, N.; Hayazawa, N.; Kawata, S.; Uosaki, K. *J. Phys. Chem. C* **2009**, *113*, 11816−11821.
(21) Li, J. F.; Huang, Y. F.; Ding, Y.; Yang, Z. L.; Li, S. B.; Zhou, Z. S.; Fan, F. R.; Zhang, W.; Zhou, Z. Y.; Wu, D. Y.; Ren, B.; Wang, Z. L.; Tian, Z. Q. *Nature* **2010**, *464*, 392−395.
(22) Butcher, D. P., Jr.; Boulos, S. P.; Murphy, C. J.; Ambrosio, R. C.; Gewirth, A. A. *J. Phys. Chem. C* **2012**, *116*, 5128−5140.
(23) Kim, K.; Shin, K. S. *Anal. Sci.* **2011**, *27*, 775−783.
(24) Hill, R. T.; Mock, J. J.; Urzhumov, Y.; Sebba, D. S.; Oldenburg, S. J.; Chen, S.-Y.; Lazarides, A. A.; Chilkoti, A.; Smith, D. R. *Nano Lett.* **2010**, *10*, 4150−4154.
(25) Nordlander, P.; Prodan, E. *Nano Lett.* **2004**, *4*, 2209−2213.
(26) Aravind, P. K.; Metiu, H. *J. Phys. Chem.* **1982**, *86*, 5076−5084.
(27) Ikeda, K.; Suzuki, S.; Uosaki, K. *Nano Lett.* **2011**, *11*, 1716−1722.
(28) Ikeda, K.; Suzuki, S.; Uosaki, K. *J. Am. Chem. Soc.* **2013**, *135*, 17387−17392.
(29) Hu, J.; Tanabe, M.; Sato, J.; Uosaki, K.; Ikeda, K. *J. Am. Chem. Soc.* **2014**, *136*, 10299−10307.
(30) Kibler, L. A.; Kleinert, M.; Randler, R.; Kolb, D. M. *Surf. Sci.* **1999**, *443*, 19−30.
(31) Ikeda, K.; Sato, J.; Uosaki, K. *J. Photochem. Photobiol., A* **2011**, *221*, 175−180.
(32) Feng, M.; Sun, H.; Zhao, J.; Petek, H. *ACS Nano* **2014**, *8*, 8644−8652.
(33) Maroun, F.; Ozanam, F.; Magnussen, O. M.; Behm, R. J. *Science* **2001**, *293*, 1811−1814.
(34) Björketun, M. E.; Karlberg, G. S.; Rossmeisl, J.; Chorkendorff, I.; Wolfschmidt, H.; Stimming, U.; Nørskov, J. K. *Phys. Rev. B: Condens. Matter Mater. Phys.* **2011**, *84*, 045407.

DOI: 10.1021/acs.nanolett.5b03093
Nano Lett. 2015, 15, 7982−7986